Journal of Molecular Liquids 320 (2020) 114222

Contents lists available at ScienceDirect

Journal of Molecular Liquids

journal homepage: www.elsevier.com/locate/molliq

Effect of glycerol on the order of the mesophase transitions of supercooled itraconazole

Kweku K. Amponsah-Efah [a], Christ Glorieux [b], Jan Thoen [b], Raj Suryanarayanan [a,*]

[a] Department of Pharmaceutics, University of Minnesota, USA
[b] Soft Matter and Biophysics Section, Department of Physics and Astronomy, KU, Leuven, Belgium

ARTICLE INFO

Article history:
Received 7 June 2020
Received in revised form 31 July 2020
Accepted 3 September 2020
Available online 12 September 2020

ABSTRACT

Itraconazole, an antifungal drug, is a thermotropic liquid crystal that exhibits nematic (N) and smectic A (SmA) phases, when cooled from the melt. By means of high-resolution adiabatic scanning calorimetry (ASC), we have obtained the temperature dependence of the heat capacity as well as the enthalpy (including latent heats) of the nematic to smectic A (N-SmA) and the isotropic to nematic (I-N) phase transitions. The N-SmA transition is weakly first-order, with substantial pretransitional heat capacity increases. The critical exponent α, obtained from power law fits to the heat capacity data, is 0.50 ± 0.05, suggesting that the N-SmA transition must be very close to a tricritical point. Indeed, with this character, the small molecule dopant glycerol (in binary mixtures with ITZ), causes interesting changes to the mesomorphic phase sequence and to the order of the phase transitions. With increasing glycerol content, the temperature width of the nematic phase systematically reduces, until a critical concentration, at which the nematic phase disappears, leading to a direct isotropic-smectic A (I-SmA) transition. The I-SmA transitions of the ITZ-glycerol mixtures show stronger first-order character with substantial latent heats and wide two-phase regions, when compared to the (N-SmA and I-N) transitions of neat itraconazole. The ability of glycerol to drive the ITZ transitions to stronger first-order character indicates a possible coupling of the additive concentration to the smectic order parameter, which leads to the development of highly ordered, stable smectic structures.

1. Introduction

Liquid crystals (LCs), have properties intermediate between crystalline solids and isotropic liquids. The rich variety of intermediate phases makes LCs excellent model systems for testing general concepts of phase transitions and critical phenomena. In particular, the first-order (discontinuous) or second-order (continuous) character of the transitions, and the universality class of critical exponents have been, and are being, the object of investigations.

Two of the most common mesophases are the nematic (N) and the smectic-A (SmA) phases [1]. In the nematic phase, rod-like molecules align parallel to each other, with their long axes all pointing approximately in the same direction. In the smectic phase, the molecules maintain the orientational order and are further organized into layers.

The nematic to smectic A (N-SmA) transition is one of the most extensively studied. Since the order in the SmA phase can be described in terms of a two-component complex order parameter, the N-SmA transition can be expected to be in the 3D–XY universality class [2,3]. Experiments have however shown non-universal critical behavior in some systems. According to the molecular field theory of McMillan and Kobayashi [4,5], as well as de Gennes [2,3], the N-SmA transition could be either first- or second-order in nature, depending on the nematic range (i.e. the temperature width of the nematic phase). A narrow nematic range indicates a strong coupling between the N and SmA order parameters, resulting in a first-order N-SmA transition. Conversely, a wide nematic range (weak coupling) gives a continuous transition. Halperin, Lubensky and Ma, via their HLM theory, however suggested that the coupling between the director fluctuations and the smectic order parameter makes the N-SmA transition always weakly first-order [6]. The isotropic-nematic (I-N) transition, usually described in terms of the Landau-de Gennes mean-field theory, or based on the Maier-Saupe theory, should be weakly first order [2,3].

Due to the wide range of complex phases that can be encountered within LC systems, as well as the different theoretical predictions about the nature of the mesomorphic transitions, experimental determination of the order of phase transitions, provides a pathway to understand the behavior of these systems. To establish the order of a phase transition, the true latent heat (or absence of latent heat) must be measured. With differential scanning calorimetry (DSC), the most popular calorimetric technique, it is possible to locate the different LC phases with sufficiently wide temperature ranges, and to qualitatively

* Corresponding author.
E-mail address: surya001@umn.edu (R. Suryanarayanan).

https://doi.org/10.1016/j.molliq.2020.114222
0167-7322/

characterize the magnitude of the thermal features associated with the transitions. DSC is however not ideally suited for confirming the order of phase transitions. This is because the latent heat and the pretransitional increase in the specific heat near a phase transition are lumped together into one thermal event (peak) [7]. Distinguishing between true latent heats and pretransitional (fluctuation induced) enthalpy variations is almost impossible, thereby making it difficult to distinguish between first- and second-order transitions [7].

Adiabatic Scanning Calorimetry (ASC), by maintaining thermal equilibrium, continuously measures the enthalpy (H) and the heat capacity (C_p) as a function of temperature. Continuous determination of $H(T)$, serves as a unique approach for confirming the order of phase transitions. An enthalpy 'jump', indicative of latent heat (ΔH_L), is a characteristic feature of a first-order (discontinuous) transition. Second-order (continuous) transitions show no discontinuities in the enthalpy ($\Delta H_L = 0$) [7,8]. However, the heat capacity, which is the temperature derivative of the enthalpy [$C_p = (\partial H/\partial T)_P$], exhibits a discontinuous jump (mean-field behavior), or a divergence (critical fluctuation behavior). Information on the pre-transitional heat capacity is also needed to analyze relevant thermal aspects of critical fluctuations [7]. With ASC, the critical behavior of different LC classes, have been studied.

Compounds (having or lacking liquid crystalline order) are added to LCs, forming binary mixtures, as a means of either (i) extending the working ranges of the mesophase transitions or (ii) exploring unusual phase sequences. It has been observed that non-mesogenic solutes broaden the I-N transition temperature leading to the subsequent formation of two-phase regions [9]. As an example, the I-N transition temperature of 5CB (a compound of the alkylcyanobiphenyl homologous series) increases, when doped with molecularly rigid carboxylic acids, but decreases when the carboxylic acid dopants have flexible aliphatic chains [10]. The transition temperatures shift without any effects on the magnitude of the total enthalpy change of the I-N transition [10]. In the case of N-SmA transitions, non-mesogenic solutes can cause a change in the order of the transition (from second- to first-order), by coupling to the order paramters [11]. Conversely, nanoparticles dispersed in liquid crystals can induce a decoupling mechanism of the order parameters, leading to a change in the critical behavior of the bulk material [12]. The unusual phase sequences that result from LC mixtures, find practical use in LC devices for display and telecommunication applications [13–15].

Itraconazole (ITZ), a pharmaceutical compound indicated for treatment of fungal infections, is a known thermotropic LC [16]. ITZ exhibits nematic and smectic phases, when cooled from the isotropic melt, with a nematic range of ~16 °C. Itraconazole is a rather unusual glassy LC, being one of the few compounds for which the smectic order can be eliminated by cooling from the isotropic phase with an appropriate rate [17]. Also, effects of addition of polymers on the smectic order of ITZ have been reported, for three different classes of polymers [18]. The polymer either disrupts the smectic order, resulting in a uniform isotropic mixture, or remains separated from the smectic domains [18]. The critical behavior of the mesophase transitions in ITZ, however, has not been studied. There is also a general interest, to know how other pharmaceutical additives affect the mesophase transitions in ITZ.

The goal of this work is therefore, to investigate the effect of glycerol, a small-molecule plasticizer [19], on the phase transitions of itraconazole. In the pharmaceutical sciences, glycerol is of interest, because it is sometimes incorporated into amorphous formulations, to aid processing [20]. Meanwhile, in the liquid crystal literature, glycerol is a typical protic solvent, used to supply mobility to amphiphilic molecules, in lyotropic LC systems [21,22]. Furthermore, when thermotropic mesogens were functionalized with glycerol (propane-2,3-diol attachments to the mesogen's aromatic core), novel thermotropic mesophases were obtained [23]. Thus, glycerol has the potential to induce unusual effects in the mesomorphic sequence of ITZ. We have investigated the thermal behavior in itraconazole, with the glycerol concentration ranging from 1 to 40% w/w. DSC studies were conducted with the goal of generating the phase diagram. We have also performed a detailed analysis of the critical behavior of the N-SmA transition of ITZ and investigated the effect of glycerol on the order of the mesophase transitions, using adiabatic scanning calorimetry.

2. Experimental methods

2.1. Materials

Itraconazole (Bepharm Limited, Shanghai, China; purity ~98%) and glycerol (Sigma Aldrich, USA, purity ≥99.5%) were used as received. All other reagents and chemicals were of analytical grade and purchased from Sigma Aldrich.

2.2. Sample preparation

Amorphous itraconazole (glass without smectic order) was prepared by melting the crystalline drug at 180 °C and rapidly cooling by dipping the melt in liquid nitrogen. To prepare ITZ-glycerol mixtures, crystalline ITZ was dissolved in dichloromethane at 50 °C with sonication, glycerol was dissolved in methanol and the two solutions were mixed. The solvent was rapidly evaporated at 50 °C under reduced pressure, in a rotary evaporator (IKA-HB10 digital system, Werke GmbH and Co. Germany) at 250 rpm, and lightly ground using a mortar and pestle, to obtain a free-flowing powder. The powder samples were further dried at room temperature under vacuum for 24 h, to remove any residual solvent, and kept in desiccators containing anhydrous calcium sulfate at −20 °C, until further use.

2.3. Differential Scanning Calorimetry (DSC)

A differential scanning calorimeter (Q2000, TA Instruments, New Castle, DE) equipped with a refrigerated cooling accessory unit was used. The instrument was calibrated (temperature, heat capacity and enthalpy) with tin, indium, and sapphire. An accurately weighed sample was hermetically sealed in an aluminum pan (T-zero®, TA Instruments) and subjected to a modulated temperature program, under dry nitrogen gas purge (50 mL/min). The temperature modulation used was ± 0.212 °C every 40 s, with an underlying heating rate of 2 °C/min.

The sample was heated from room temperature (~20 °C) to 180 °C, held for ~1 min to ensure complete melting, cooled back to room temperature and reheated to the melting temperature. Both the heating and cooling rates were 2 °C/min.

DSC data analysis was performed with Universal Analysis® software (TA Instruments). In the text, glass transition temperatures (T_g) are reported as the midpoint of the baseline shift (step-change) in the reversing heat flow signals. Phase transition temperatures are evaluated from the peak positions of the endothermic or exothermic reversing heat flow signals. Enthalpy change values are the peak areas of the reversing heat flow endo or exotherms.

2.4. Adiabatic Scanning Calorimetry (ASC)

High-resolution enthalpy and heat capacity data were obtained with a novel Peltier-element-based implementation of the adiabatic scanning calorimetry concept (pASC). The modes of operation are described in detail elsewhere [24,25]. An accurately weighed sample (~50 mg) was placed in a 120 μL stainless steel medium-pressure DSC crucible (Mettler-Toledo GmbH, Switzerland). The sample was heated from room temperature to ~190 °C, held for ~1 min to ensure complete melting, and rapidly cooled back to room temperature. The resulting glass was again reheated rapidly to ~60 °C, after which a very slow average scan rate (on the order of 50 mK/min; details in the text) was imposed while the ASC data were collected in the 60–100 °C region. This sequence was necessary (i) to ensure the samples did not crystallize

during the run, and (ii) to ensure a standardized thermal history for the samples.

3. Brief theory of adiabatic scanning calorimetry

Adiabatic scanning calorimetry measures with high resolution, the heat capacity and enthalpy near critical points in soft matter systems (e.g. liquid mixtures and liquid crystals) [1,26]. A constant, known heating or cooling power is applied to the sample cell (differently from imposing a constant rate, as done in DSC-type calorimeters) with an adiabatic shield that follows the temperature evolution of the sample cell. During a run, the sample temperature $T(t)$ is recorded as a function of time t, and the heat capacity $C_p(T)$ as a function of temperature is calculated via the ratio of the known constant power P and the changing temperature rate $\dot{T} = \mathrm{d}T/\mathrm{d}t$:

$$C_p(T) = \frac{P}{\dot{T}} \tag{1}$$

This leads to a continuous heat capacity curve. The heat capacity of the addenda $C_{add}(T)$, obtained in a separate calibration experiment, is subtracted from $C_p(T)$ in order to obtain the heat capacity of the bare sample. The result is divided by the sample mass to arrive at the specific heat capacity of the sample. The same $T(t)$ data and the known constant power P directly result in the continuous enthalpy curve $H(T)$, since

$$H(T) - H(T_0) = \int_{t_0}^{t(T)} P\,dt = P(t - t_0) \tag{2}$$

where $H(T_0)$ is the enthalpy of the system at the starting time t_0 of the experiment. The constant power results in the simple solution of the integral. The enthalpy of the sample is obtained after subtraction of the enthalpy of the addenda obtained from the calibration experiment. Further division by the sample mass results in the specific enthalpy.

In an ASC run, the power P is kept constant in Eq. (1) and the resulting *changing* rate $\dot{T}$ is measured. This is exactly the opposite of what is done in DSC; in DSC, a predetermined constant rate (usually large for resolution reasons) is applied, and the *changing* power $P(t)$ is measured (differentially). Also, in ASC, at a transition, the rate reduces almost effectively to zero, which ensures thermal and thermodynamic equilibrium. In DSC however, it becomes more and more challenging to deliver (at the right temperature) the strongly increasing power needed to maintain the imposed temperature rate. This results in rounding off and overshooting phenomena.

An essential requirement of high-resolution ASC operating in a (slow) heating mode is the equality (mK or better) of the temperatures of the adiabatic shield and of the sample holder in very weak thermal contact with this adiabatic shield. The temperature of the adiabatic shield is maintained at the temperature of the sample holder by means of a proportional-integrating feedback loop that controls electrical heating of the shield. In cooling mode, a constant (preset) temperature difference between sample and shield must be maintained within the same stability limits. To achieve this, highly sensitive thermistors (placed on the sample holder and shield), requiring careful and extensive calibrations, have been used in the past. However, differences in the temperature coefficients of the thermistors, made measurements over large temperature ranges very complicated. In the recent Peltier-element-based implementation, pASC, these problems are completely eliminated [24,25]. This is achieved by inserting a highly sensitive semiconductor-material-based Peltier element, to detect (and next nullify) the temperature difference between sample and shield.

4. Results and discussion

4.1. General information on itraconazole

Itraconazole (ITZ) is a crystalline powder, that melts at 168 °C [16,18]. When cooled from the melt, the isotropic (I) liquid transforms, first to a nematic (N) phase, and then to a smectic A (SmA) phase, before vitrifying. The LC transitions are reversible upon reheating. The isotropic melt is light yellow and transparent. However, a visible colour-change (white, opaque) occurs at the I-N transition temperature, which is retained upon vitrification. Phase assignments based on differential scanning calorimetry and X-ray diffractometry, have been reported in the literature [16,18,27,28].

4.2. Effect of glycerol on the mesophase transitions

Glycerol was incorporated into itraconazole, via the solvent evaporation technique, commonly used to make amorphous solid dispersions. Homogeneous itraconazole-glycerol mixtures were prepared up to a glycerol content of 40% w/w, beyond which the material became sticky and visibly phase-separated. The binary mixtures with glycerol content <30% w/w were free-flowing powders.

To systematically characterize the phase transitions, under a "standardized" thermal history, each solvent-evaporated formulation was first melted in situ, in the DSC pan, cooled to room temperature at ~2 °C/min, and reheated at the same rate. Representative reheating scans of select compositions are shown in Fig. 1, with the corresponding transition temperatures and enthalpies listed in Table 1. A phase diagram constructed based on the DSC results, is presented in Fig. 2.

The mesophase transition temperatures for neat itraconazole, are pointed out in the topmost scan of Fig. 1a. The glass (T_g), nematic-to-smectic A (T_{N-SmA}), and isotropic-to-nematic (T_{I-N}) transitions, occur at ~59, 74 and 90 °C respectively. These transition temperature values and enthalpy changes (Table 1, 0% glycerol) are in agreement with the literature values [16,27,28].

As the glycerol content increases from 0 to 2% w/w, the temperature of the nematic-to-smectic A transition (T_{N-SmA} ≈74 °C, for neat itraconazole) does not change appreciably, indicating that the smectic state is not destabilized by the additive. The isotropic-to-nematic transition temperature (T_{I-N} ≈90 °C, in neat itraconazole) however, systematically shifts to lower values. At glycerol concentrations ≥5% w/w, the nematic phase completely disappears, indicating a direct isotropic ➔ smectic A (I-SmA) transition. The I-SmA transition is also temperature-invariant, with increasing glycerol concentration (Fig. 1b; Table 1, 5–40% glycerol).

The enthalpy changes of the mesophase transitions are also affected by the additive. As the glycerol content increases from 0% to 2% w/w, the enthalpy change of the nematic-to-smectic transition (ΔH_{N-SmA}) increases, while that of the nematic-to-isotropic transition (ΔH_{I-N}) decreases (Table 1). The I-SmA transition endotherms (observed in compositions with ≥5% w/w glycerol), are however noticeably pronounced. Of note, the ΔH_{I-SmA} at any composition, is much higher, than the sum of ΔH_{I-N} and ΔH_{N-SmA} (observed at glycerol concentrations ≤2% w/w).

Generally, condensation from the isotropic to the nematic phase (I-N) requires calamitic molecules to reorient with their molecular axes approximately parallel to the nematic director. This typically manifests as a larger change in enthalpy, than transition from the nematic to the smectic A phase (N-SmA), which only requires longitudinal displacement of the molecules to form layers (in fact only weak density modulations along the director) [7,8]. Direct transition from the isotropic to the smectic A phase (I-SmA), on the other hand, typically goes along with a pronounced enthalpy change [7,29]. This is because, in order to complete the I-SmA transition, a significant increase in orientational as well as translational order must occur almost simultaneously.

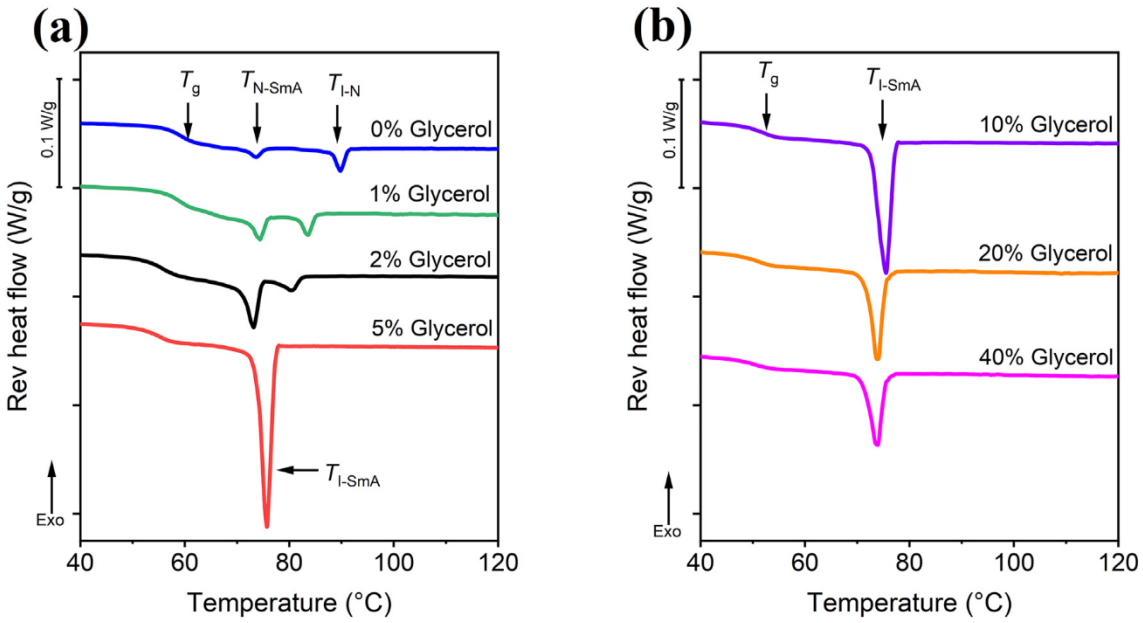

Fig. 1. DSC heating curves of itraconazole-glycerol binary mixtures of different compositions. The glycerol content (w/w) is given above each curve. (a) 0 to 5% glycerol, and (b) 10 to 40% glycerol. Each sample was heated from room temperature (~20 °C) to 180 °C, held for 1 min, and cooled back to room temperature. The sample was then reheated to 180 °C. Both the heating and cooling rates were 2 °C/min. Only the final heating curves over the temperature range of interest, are shown.

Often, when a mesogenic material possesses intermediate phases, the individual enthalpy changes of the low-ordered phases sum up to the total enthalpy change for the higher ordered phase [29]. Thus, the enthalpy change of the I-N and N-SmA phases are expected to sum up to the total enthalpy change of the I-SmA transition. However, as shown in Table 1, the ΔH_{I-SmA} values are substantially higher. This unusual finding indicates that the ITZ molecules become exceptionally well-ordered, with 5–10% glycerol being the most favorable composition.

4.3. Effect of glycerol on the glass transition temperature

The glass transition temperature (T_g) decreases only slightly, as the glycerol content increases (Figs. 1 and 2; Table 1). Glycerol, due to its low T_g (~−83 °C), is usually a potent plasticizer of amorphous pharmaceuticals. To assess the extent of plasticization, the experimentally determined T_g values, are compared with the values predicted by the Gordon-Taylor (GT) additivity rule for binary mixtures [30–33] (Eq. (3)).

$$T_{gx} = \frac{T_{g1}w_1 + K(T_{g2}w_2)}{w_1 + Kw_2} \tag{3}$$

The subscripts 1 and 2 represent the components itraconazole and glycerol respectively, and w is the weight fraction of each component. K is a constant, calculated with the Simha–Boyer rule [31].

$$K \cong \frac{\rho_1 T_{g1}}{\rho_2 T_{g2}} \tag{4}$$

where ρ_1 and ρ_2 are the densities of itraconazole (1.4 g/cm^3) and glycerol (1.26 g/cm^3) respectively.

The GT relation assumes perfect volume additivity at T_g and no interactions between the two components [33]. As shown in Fig. 3, a consistent positive deviation from the trend predicted by the GT equation, is observed for mixtures, indicating a reduction in the net free volume and hence, a more efficient packing of the itraconazole molecules [34].

4.4. The order of the transitions

In the context of this investigation, three types of phase transitions are relevant: the isotropic-nematic (I-N), the nematic-smectic A (N-SmA) and the isotropic-smectic A (I-SmA). For purely geometrical reasons (regarding molecular orientation), the I-N transition must be first-order (with the possible exception at a single critical point induced by an external parameter) [3]. On the same grounds (because

Table 1
Transition temperatures (T, °C) and associated enthalpies (ΔH, J/g) determined from the reversible heat flow signals of modulated DSC reheating scans (at 2 °C/min). Each value is an average of three replicate runs with standard deviations in parentheses. The McMillan ratios (T_{N-SmA}/T_{I-N}) are included for the samples with 0 to 2% glycerol content.

Glycerol content (w/w)	Isotropic – nematic		Nematic–smectic A		Isotropic – smectic A		Smectic A – glass	$\frac{T_{N-SmA}}{T_{I-N}}$
	T, °C	ΔH, J/g	T, °C	ΔH, J/g	T, °C	ΔH, J/g	T_g, °C	
0%	89.8 (0.1)	1.6 (0.2)	73.7 (0.3)	0.6 (0.1)	–	–	59.3 (0.6)	0.955
1%	83.7 (0.0)	1.2 (0.1)	74.4 (0.1)	1.9 (0.2)	–	–	59.3 (0.5)	0.973
2%	80.0 (1.7)	0.9 (0.3)	73.2 (0.1)	3.7 (0.2)	–	–	55.6 (0.8)	0.980
5%	–	–	–	–	75.3 (0.4)	11.7 (1.3)	55.5 (0.5)	–
7%	–	–	–	–	75.9 (0.0)	9.8 (0.5)	55.2 (2.9)	–
10%	–	–	–	–	75.5 (0.5)	10.1 (1.1)	52.4 (0.9)	–
20%	–	–	–	–	73.1 (0.7)	8.0 (0.8)	51.2 (0.2)	–
30%	–	–	–	–	73.1 (0.6)	7.8 (0.3)	51.5 (0.2)	–
40%	–	–	–	–	73.9 (0.2)	5.7 (0.2)	50.0 (0.7)	–

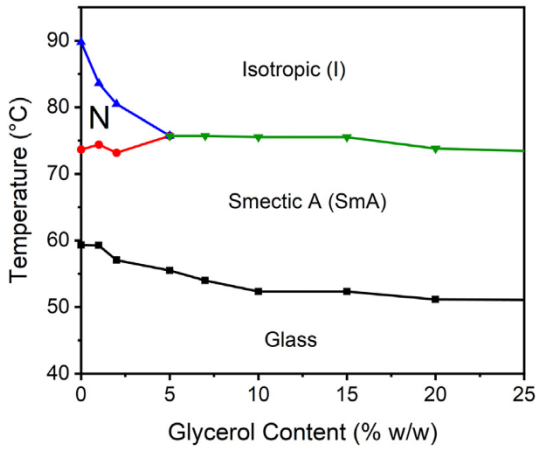

Fig. 2. Phase diagram generated from the DSC results (Fig. 1;Table 1). Solid lines are drawn to assist in assessing the trends. N = nematic phase.

orientational order is also present in the SmA phase), the I-SmA transition should be first-order.

There are no obvious reasons, however, for the N-SmA transition to be first- or second-order. Extensive calorimetric investigations of the N-SmA transition have been carried out [7]. It has been found that the temperature range of the nematic phase (i.e. the temperature width between the I-N and N-SmA transitions) plays an important role. Compounds with narrow nematic ranges are more likely to exhibit first-order N-SmA transitions, while second-order transitions are encountered for compounds with wide nematic ranges [2–5]. This behavior is often qualitatively characterized by the McMillan phenomenological parameter, $r = T_{SmA-N}/T_{N-I}$ (ratio of absolute temperatures) [5]. According to McMillan's model the N-SmA transition is first-order for $r > 0.87$, but second-order for values below 0.87. Experimentally, first-order transitions have only been observed for McMillan ratios close to 1, typically above 0.95 [7,35]. From the variation in McMillan parameter and differences in total transition enthalpies (ΔH in Table 1), there is some indication for differences in the order of the transition for the itraconazole samples having different glycerol contents. Therefore, in the following sections, we analyze Adiabatic Scanning Calorimetry (ASC) data to establish the nature of the N-SmA transition of the itraconazole samples with different glycerol contents.

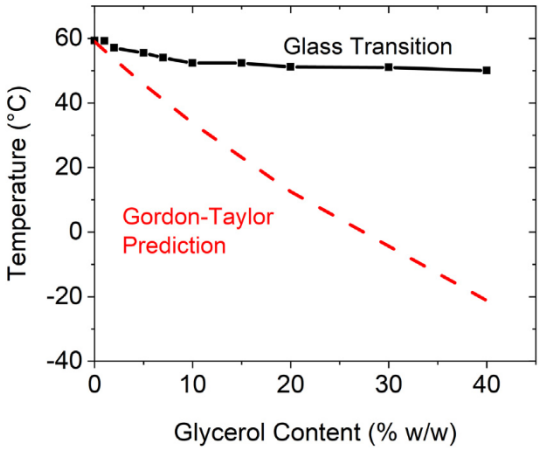

Fig. 3. Experimental glass transition temperatures (T_g) of itraconazole-glycerol binary mixtures, compared with the values predicted using the Gordon-Taylor equation.

4.5. ASC results for neat itraconazole

Fig. 4a shows an overview of the temperature dependence of the specific heat capacity C_p and the specific enthalpy H from well below the smectic A (SmA) to well into the isotropic (I) phase. For the sake of clear contrast, a large, linearly temperature-dependent enthalpy background has been subtracted from the measured enthalpy values. Indeed, for a constant heat capacity, the enthalpy increase is linearly dependent on temperature. Subtracting such (often irrelevant) contribution allows a more detailed study of fine phase transition effects. Furthermore, a careful inspection of the enthalpy and heat capacity, as well as higher order derivatives, allows the temperature width of the (impurity induced) two-phase region to be located, and the true latent heats to be separated from (often substantial) pretransitional effects. This treatment was applied to all the samples, and the transition temperatures and latent heats are summarized in Table 2. The transition temperatures and total enthalpy changes (ΔH) measured by adiabatic scanning calorimetry, for all the samples (Table 2) are in agreement with the corresponding values obtained via DSC (Table 1).

We first describe the N-SmA transition for neat itraconazole. In Fig. 4b, the temperature scale of the $H(T)$ data is expanded (within 2 °C temperature range), to show the detailed behavior very close to the N-SmA transition. A linear change in enthalpy with an almost constant effective heat capacity (constant slope) can be identified between the two dashed vertical lines, over a temperature interval of 0.15 ± 0.03 °C. This allows a small but finite latent heat of 0.095 ± 0.010 J/g, to be identified, indicating that the N-SmA transition is weakly first-order.

Similar analyses of the $H(T)$ data were performed around the isotropic-to-nematic (I-N) transition. A larger latent heat of 0.27 ± 0.02 J/g can be separated from the total enthalpy change (see Table 2), confirming a stronger first-order nature, for the I-N transition.

It is clear (from the profiles in Fig. 4), that for both transitions (N-SmA and I-N), there are large pretransitional contributions to the total enthalpy changes. These aspects will be discussed in a separate section.

4.6. ASC results for the ITZ-glycerol mixtures

Fig. 5a (similar to Fig. 4) gives an overview of the temperature dependence of the specific heat capacity C_p and the specific enthalpy H from well below the smectic A (SmA) to well in the isotropic phase, for the ITZ + 2% glycerol mixture. Compared to neat ITZ, the I-N transition occurs at a lower temperature (80.4 °C), while the N-SmA transition temperature (72.7 °C) remains almost unaffected, resulting in a much narrower nematic range (i.e. $T_{I-N} - T_{N-SmA} = 7.7$ °C). Both transitions are clearly first-order, with substantial (true) latent heats (see Table 2; 2% glycerol). Additionally, some pretransitional specific heat capacity increases and minor supercooling are observed.

When the glycerol content is increased to 5% w/w, however, only one strongly first-order transition, with substantial total enthalpy increase and a large true latent heat over a wide two-phase region, is observed (see Fig. 5b and Table 2). The I-SmA transition also shows some pretransitional heat capacity increase in the SmA phase.

4.7. Critical exponent analysis of the N-SmA transition

Second-order (continuous) phase transitions are characterized by large fluctuations, which, for a properly defined order-parameter, diverge in size to infinity. This size divergence can be described by a power law, with a characteristic critical exponent depending on the universality class of the phase transition [36]. The limiting behavior of the specific heat capacity at a second-order transition, can also be described by means of a power law of the form:

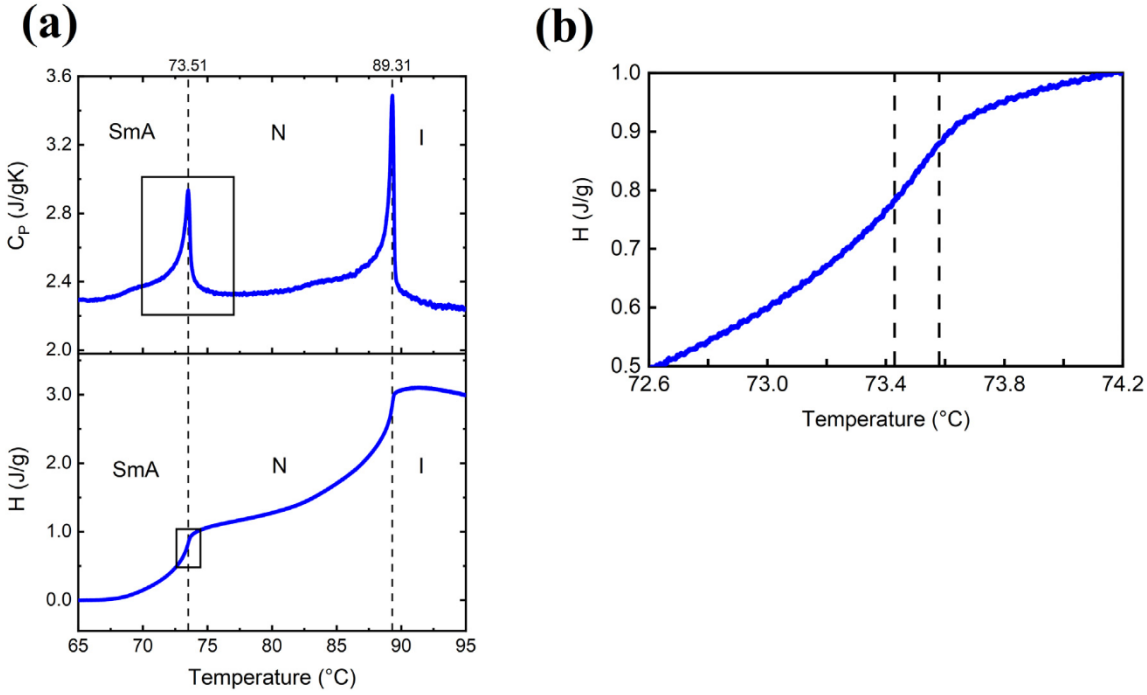

Fig. 4. (a) ASC of neat itraconazole, covering the N-SmA and the I-N transitions. The upper panel displays the specific heat capacity and the bottom panel the specific enthalpy as a function of temperature. Dashed lines are the mesophase transition temperatures. A linear temperature-dependent background, $2.3(T - T_{ref})$, with T_{ref} an arbitrary reference temperature, has been subtracted from the direct enthalpy results. (b) A blow-up of the small square in the bottom panel a. The vertical dashed lines indicate a two-phase region (between T=73.43 °C and T= 73.58 °C).

$$C_p = A|\tau|^{-\alpha} + B \tag{5}$$

with $\tau = (T - T_c)/T_c$. The parameter A is the critical amplitude, α is the critical exponent, T_c is the critical temperature (T and T_c in kelvin) and B is the background term. The different coefficients in Eq. (5) must be derived from (non-linear) least-squares fitting of experimental data. However, the fact that ASC scans result directly in an enthalpy $H(T)$ curve (see Eq. (2)) allows substantial simplification. One can define the following quantity:

$$C = \frac{H - H_c}{T - T_c} \tag{6}$$

which corresponds to the slope of the chord connecting $H(T)$ at T, with H_c at T_c. It can easily be shown, that C has a power law behavior of the form [1,7]:

$$C = \frac{A}{1-\alpha}|\tau|^{-\alpha} + B \tag{7}$$

Both C_p and C have the same critical exponent, and either Eqs. (5) or (7) can be used in fitting data to arrive at important values for the critical exponent α and amplitude A. However, by considering the difference $(C - C_p)$, above or below T_c, the (unimportant) background term drops out, resulting in:

$$C - C_p = \frac{\alpha A}{1-\alpha}|\tau|^{-\alpha} \tag{8}$$

Taking the logarithm on both sides of Eq. (8) gives:

$$\log(C - C_p) = \log\left(\frac{\alpha A}{1-\alpha}\right) - \alpha \log|\tau| \tag{9}$$

As a result, one obtains a straight line with a negative slope immediately giving the critical exponent α.

In Fig. 6, data for the two quantities C and C_p are given for the N-SmA transition of neat itraconazole. The corresponding logarithmic plot [see Eq. (9)] is given in Fig. 7. From the detailed analysis of the enthalpy and heat capacity curves, and their higher derivatives, we arrived at a two-phase region of 150 ± 30 mK and a small latent heat of 0.095 ± 0.010 J/g. Since the power law description breaks down in the two-phase region, only data outside that region are used in Figs. 6 and 7. From the limiting slope of the data (for $\log|\tau| < -2.5$) in Fig. 7, a value for α of 0.50 ± 0.05 can be estimated above and below the transition. The deviations from the straight line observed for $\log|\tau| > -2.5$,

Table 2
Adiabatic scanning calorimetry results for itraconazole with different glycerol contents. The transition temperature (T, °C), total enthalpy change over the transition (ΔH, J/g), and true latent heat (ΔH_L, J/g) are measured during a heating run with constant power, resulting in slow average scanning rate, on the order of 50 mK/min for full measuring ranges. For a complete definition of all the terms, see reference [1,24,25].

Glycerol content (w/w)	Isotropic – nematic			Nematic–smectic A			Isotropic – smectic A			$\frac{T_{N-SmA}}{T_{I-N}}$
	T (°C)	ΔH (J/g)	ΔH_L (J/g)	T (°C)	ΔH (J/g)	ΔH_L (J/g)	T (°C)	ΔH (J/g)	ΔH_L (J/g)	
0%	89.31 ± 0.03	1.61 ± 0.05	0.27 ± 0.02	73.51 ± 0.03	0.76 ± 0.05	0.095 ± 0.010	–	–		0.956
2%	80.41 ± 0.02	0.87 ± 0.05	0.13 ± 0.03	72.71 ± 0.05	3.2 ± 0.2	0.61 ± 0.03	–	–		0.978
5%	–	–	–		–		75.6 ± 0.1	11.8 ± 0.5	4.8 ± 0.2	

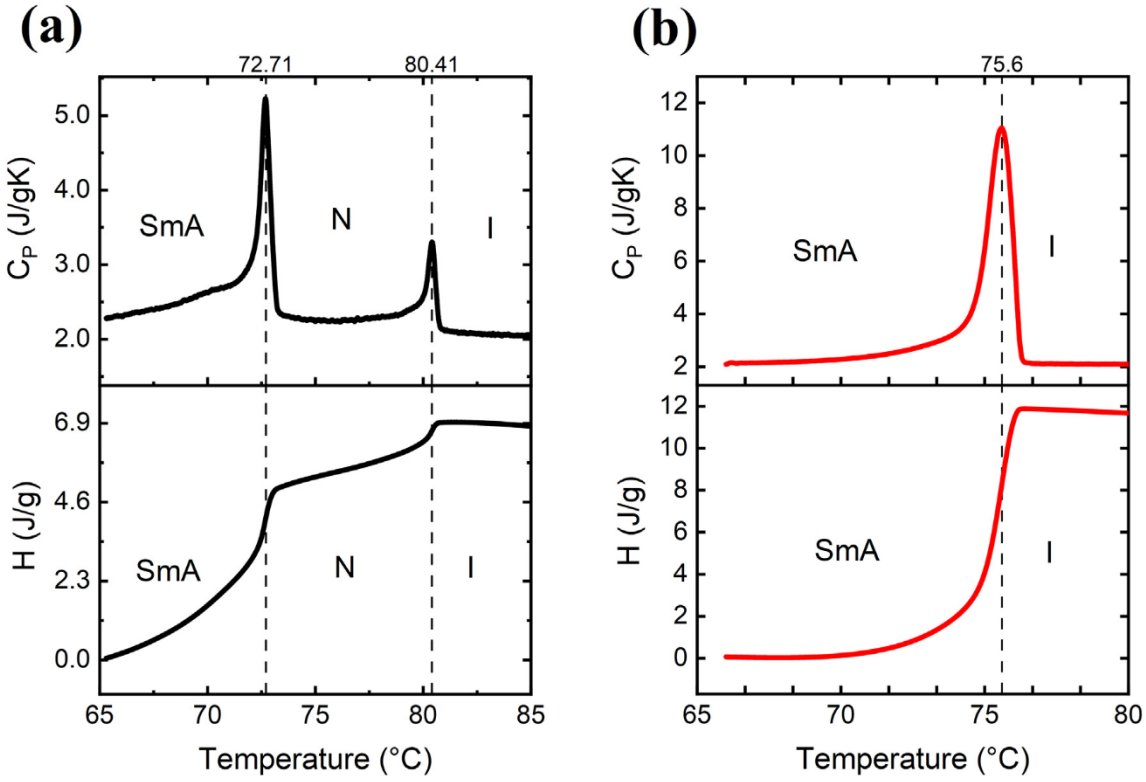

Fig. 5. ASC results for ITZ-glycerol mixtures from the smectic A to the isotropic phase. The upper panel shows the specific heat capacity and the bottom panel the specific enthalpy as a function of temperature. For the sake of clarity, a linear temperature-dependent background has been subtracted from the direct enthalpy results. (a) ITZ + 2% w/w glycerol; background $2.7(T - T_{ref})$. (b) ITZ + 5% w/w glycerol; background $2.2(T - T_{ref})$. T_{ref} is an arbitrary reference temperature.

can be ascribed to higher order correction terms, relevant away from the transition, which have been neglected in Eqs. (5) and (7).

Although the N-SmA transition in neat itraconazole is weakly first-order, the small value of the latent heat and the consistency of the obtained value of critical exponent α with the tricritical value $\alpha = 0.5$, indicates the N-SmA transition is close to a tricritical point.

For the mixture of itraconazole with 2% of glycerol, although a N-SmA transition (with a much smaller nematic range) is observed, a substantial true latent heat (0.61 ± 0.03 J/g), in addition to pretransitional contributions, is also present for this transition. Moreover, the transition is broadened over several tenths of a degree, not allowing a similar critical exponent analysis as for neat itraconazole. Nevertheless, the substantial latent heat, the narrower nematic range and a McMillan parameter closer to 1 (Table 2; 2% glycerol), are fully consistent with the overall picture of the nature of the nematic-to-smectic A transitions.

For the isotropic-to-nematic (I-N) transitions observed for neat itraconazole and itraconazole +2% glycerol, as well as for the isotropic-to-smectic A (I-SmA) transition for itraconazole +5% glycerol, sizeable true latent heats (with wide two-phase regions) and pretransitional contributions are observed (see Table 2). Unfortunately, the widths of the two-phase regions do not allow a reliable analysis of the pretransitional contributions.

4.8. Implications of the critical behavior

The critical exponent analysis and the extracted magnitudes of the latent heats, confirm the general picture concerning the three transitions investigated. The N-SmA transition in ITZ, being close to a tricritical point, is easily driven from a weakly first-order transition, to a (strongly) first-order transition, most likely due to a coupling of the concentration of glycerol to the nematic and smectic order parameters. The invariance of the resulting I-SmA transition temperature to increasing glycerol concentration, the exceptionally large total enthalpy change, and the large latent heats of the I-SmA transition, all point to ITZ-glycerol mixtures having highly ordered, rigid smectic layers. Structural, molecular orientation, and molecular interaction studies from scattering and spectroscopy experiments, will be needed to provide additional insight into the smectic ordering process of the binary mixtures, and to arrive at the most likely packing arrangement. This will be the subject of a different manuscript.

4.9. Significance

Glassy liquid crystals are versatile materials, with wide range of applications from displays, to organic electronics. This study demonstrates that glycerol (and by extension, other similar small-molecule

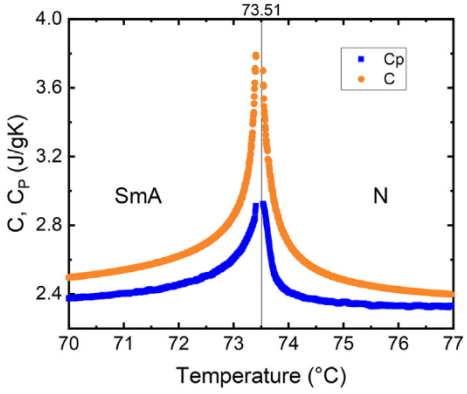

Fig. 6. Adiabatic scanning calorimetry results above and below the N-SmA transition of neat itraconazole. The lower (blue) curves are the specific heat capacity C_p values, a blow up of the square in the top panel of Fig. 4a. The upper (orange) curves are results for the quantity C defined in Eq. (6).

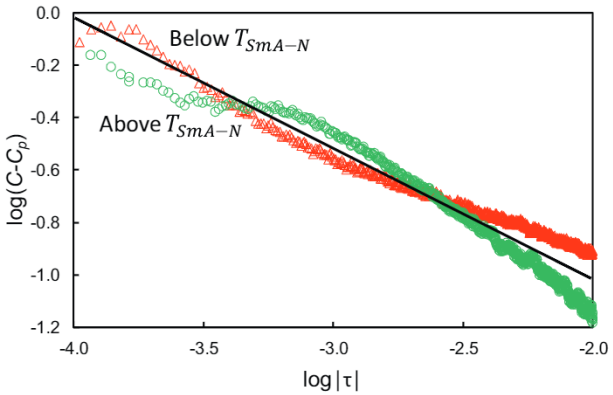

Fig. 7. Adiabatic scanning calorimetry results for the N-SmA transition of neat itraconazole. Double logarithmic plot of the difference $(C - C_p)$ expressed in J/gK, as a function of the reduced temperature difference $|\tau|$. Red triangles are for $T < T_c$ and green circles for $T > T_c$. The average limiting slope of the black solid line, is consistent with α=0.50 ± 0.05.

plasticizers, such as water or ethylene glycol) can be incorporated at very low concentrations to modulate the thermotropic phase sequence and to increase the stability of the smectic-A layers. In the model compound studied, this wide range of tunability is linked to the fact that the N-SmA transition is close to a tricritical point. A coupling of the concentration of glycerol to the smectic order parameter, drives the N-SmA transition from a weak to a strong first-order character. Beyond a critical additive concentration, the nematic phase can be eliminated. This relatively simple approach of incorporating a small molecule plasticizer via solvent evaporation, into a glassy thermotropic LC, presents an opportunity to systematically modulate phase behavior in smectic phases.

Since the smectic phase possesses a lower free energy level than the amorphous phase, pharmaceutical thermotropic LCs with stabilized smectic phases may be more resistant to crystallization, while offering adequate dissolution enhancement, when compared to the corresponding crystalline drug. The stabilized smectic phase therefore presents an alternate formulation approach for improving the bioavailability of pharmaceutical compounds with poor aqueous solubility.

5. Conclusions

We have investigated the effects of glycerol, a small molecule dopant, on the phase behavior of the thermotropic liquid crystal, itraconazole. A phase diagram was constructed from DSC heating curves, by varying the concentration of glycerol from 1 to 40% w/w. When cooled from the melt, the isotropic liquid of neat itraconazole transitions to the nematic (N) state, and then to the smectic A (SmA) state, before vitrifying.

With increasing glycerol content, the I-N transition shifts to lower temperatures without substantial modification of the N-SmA transition temperature. At glycerol contents ≥5% w/w, however, the nematic phase disappears, indicating a direct I-SmA transition. The I-SmA transition enthalpy is significantly larger than the individual I-N and N-SmA transition enthalpies.

We also performed heat capacity and enthalpy measurements around the phase transitions, with high resolution adiabatic scanning calorimetry. The N-SmA transition in neat itraconazole shows the characteristics of a weakly first-order transition, with a small latent heat of 0.095 ± 0.010 J/g. From a detailed analysis of the critical pretransitional behavior, an effective heat capacity critical exponent of 0.50 ± 0.05 is obtained, in agreement with predictions of the Landau-de Gennes mean-field theory for tricritical behavior.

As expected, the I-N transition in ITZ is found to be first-order with a larger latent heat. The transitions observed in the ITZ-glycerol binary mixtures, however, show stronger first-order character (when compared to those in neat ITZ), with sizeable true latent heats, and pre-transitional contributions.

CRediT authorship contribution statement

Kweku K. Amponsah-Efah: Conceptualization, Methodology, Investigation, Writing, Reviewing, Editing.

Christ Glorieux: Conceptualization, Methodology, Investigation, Writing, Reviewing, Editing (section of Adiabatic Scanning Calorimetry).

Jan Thoen: Conceptualization, Methodology, Investigation, Writing, Reviewing, Editing (section of Adiabatic Scanning Calorimetry).

Raj Suryanarayanan: Conceptualization, Methodology Writing, Reviewing and Editing, Resources, Project administration, Funding acquisition, Supervision.

Declaration of competing interest

The authors declare that they have no known competing financial interests or personal relationships that could have appeared to influence the work reported in this paper.

Acknowledgements

This project was funded by the National Science Foundation (grant award number NSF-CMMI-1662039). The support of the William and Mildred Peters endowment fund is acknowledged. KKAE acknowledges the Bighley Graduate Student Fellowship. We also thank Dr. Jorge Vinals and Dr. Satyendra Kumar for enlightening discussions.

References

[1] J. Thoen, H. Marynissen, W. Van Dael, Temperature dependence of the enthalpy and the heat capacity of the liqud-crystal octylcyanobiphenyl (8CB), Phys. Rev. A 26 (5) (1982) 2886–2905.

[2] P.G. de Gennes, An analogy between superconductors and smectics A, Solid State Commun. 10 (9) (1972) 753–756, https://doi.org/10.1016/0038-1098(72)90186-X.

[3] P.G. de Gennes, J. Prost, The Physics of Liquid Crystals, Second Oxford University Press, 1993.

[4] K.K. Kobayashi, On the theory of translational and orientational melting with application to liquid crystals, Phys. Lett. A 31 (3) (1970) 125–126, https://doi.org/10.1016/0375-9601(70)90186-6.

[5] W.L. McMillan, Simple molecular model for the Smectic a phase of liquid crystals, Phys. Rev. A 4 (3) (1971) 1238–1246, https://doi.org/10.1103/PhysRevA.4.1238.

[6] B.I. Halperin, T.C. Lubensky, S. Ma, First-order phase transitions in superconductors and smectic-a liquid crystals, Phys. Rev. Lett. 32 (6) (1974) 292–295, https://doi.org/10.1103/PhysRevLett.32.292.

[7] J. Thoen, Thermal investigations of phase transitions in thermotropic liquid crystals, Int. J. Mod. Phys. B 09 (18n19) (1995) 2157–2218, https://doi.org/10.1142/S0217979295000860.

[8] S. Kumar, in: S. Kumar (Ed.), Liquid Crystals: Experimental Study of Physical Properties and Phase Transitions, Cambridge University Press, Cambridge, 2001.

[9] P.K. Mukherjee, B.C. Khan, Nematic to smectic-a phase transition in mixture of liquid crystal and nonmesogenic impurities: existence of tricritical point, Liq. Cryst. 46 (7) (2019) 1060–1066, https://doi.org/10.1080/02678292.2018.1555722.

[10] V. Jirón, E. Castellón, Increased nematic–isotropic transition temperature on doping a liquid crystal with molecularly rigid carboxylic acids, J. Phys. Chem. B 124 (5) (2020) 890–899, https://doi.org/10.1021/acs.jpcb.9b09567.

[11] P.K. Mukherjee, Effect of nonmesogenic solute on the nematic-smectic-a phase transition, J. Chem. Phys. 116 (21) (2002) 9531–9536, https://doi.org/10.1063/1.1476314.

[12] S. Diez-Berart, D.O. López, M.R. de la Fuente, J. Salud, M.A. Pérez-Jubindo, D. Finotello, Critical behaviour in liquid-crystalline phase transitions: a comparative study of 9OCB in bulk and anopore membranes, Liq. Cryst. 37 (6–7) (2010) 893–901, https://doi.org/10.1080/02678291003798156.

[13] D. Pauluth, K. Tarumi, Advanced liquid crystals for television, J. Mater. Chem. (2004) https://doi.org/10.1039/b400135b.

[14] J.C. Jones, The fiftieth anniversary of the liquid crystal display, Liq. Cryst. Today 27 (3) (2018) 44–70, https://doi.org/10.1080/1358314X.2018.1529129.

[15] C. Tschierske, Liquid crystal engineering - new complex mesophase structures and their relations to polymer morphologies, nanoscale patterning and crystal engineering, Chem. Soc. Rev. 36 (12) (2007) 1930–1970, https://doi.org/10.1039/b615517k.

[16] K. Six, G. Verreck, J. Peeters, K. Binnemans, H. Berghmans, P. Augustijns, R. Kinget, G. Van den Mooter, Investigation of thermal properties of glassy itraconazole: identification of a monotropic mesophase, Thermochim. Acta 376 (2) (2001) 175–181, https://doi.org/10.1016/S0040-6031(01)00563-9.

[17] R. Teerakapibal, C. Huang, A. Gujral, M.D. Ediger, L. Yu, Organic glasses with tunable liquid-crystalline order, Phys. Rev. Lett. 120 (5) (2018) 1–5, https://doi.org/10.1103/PhysRevLett.120.055502.
[18] A. Kozyra, N.A. Mugheirbi, K.J. Paluch, G. Garbacz, L. Tajber, Phase diagrams of polymer-dispersed liquid crystal systems of itraconazole/component immiscibility induced by molecular anisotropy, Mol. Pharm. 15 (11) (2018) 5192–5206, https://doi.org/10.1021/acs.molpharmaceut.8b00724.
[19] A. Marcilla, M. Beltran, Mechanisms of plasticizer action, in: G. Wypych (Ed.), Handbook of Plasticizers, ChemTec Publishing, Toronto 2017, pp. 119–134, https://doi.org/10.1016/B978-1-895198-97-3.50007-X.
[20] J.S. LaFountaine, J.W. McGinity, R.O. Williams, Challenges and strategies in thermal processing of amorphous solid dispersions: a review, AAPS PharmSciTech 17 (1) (2016) 43–55, https://doi.org/10.1208/s12249-015-0393-y.
[21] B.M. Carter, B.R. Wiesenauer, E.S. Hatakeyama, J.L. Barton, R.D. Noble, D.L. Gin, Glycerol-based bicontinuous cubic lyotropic liquid crystal monomer system for the fabrication of thin-film membranes with uniform nanopores, Chem. Mater. 24 (21) (2012) 4005–4007, https://doi.org/10.1021/cm302027s.
[22] M. Kölbel, T. Beyersdorff, C. Tschierske, S. Diele, J. Kain, Thermotropic and lyotropic liquid crystalline phases of rigid aromatic amphiphiles, Chem. - A Eur. J. 6 (20) (2000) 3821–3837, https://doi.org/10.1002/1521-3765(20001016)6:20<3821::AID-CHEM3821>3.0.CO;2-8.
[23] P. Fuchs, C. Tschierske, K. Raith, K. Das, S. Diele, A thermotropic mesophase comprised of closed micellar aggregates of the normal type, Angew. Chemie Int. Ed. 41 (4) (2002) 628–631, https://doi.org/10.1002/1521-3773(20020215)41:4<628::AID-ANIE628>3.0.CO;2-I.
[24] Thoen, J.; Leys, J.; Glorieux, C. Adiabatic Scanning Calorimeter. European Patent: EP 2 91328 B1(Sept. 02, 2015), US Patent: US 9.310.263 B2 (April 12, 2016).
[25] J. Leys, P. Losada-Pérez, C. Glorieux, J. Thoen, Application of a novel type of adiabatic scanning calorimeter for high-resolution thermal data near the melting point of gallium, J. Therm. Anal. Calorim. 117 (1) (2014) 173–187, https://doi.org/10.1007/s10973-014-3654-1.
[26] J. Thoen, E. Bloemen, H. Marynissen, W. Van Deal, High-resolution calorimetric investigations of phase transitions in liquids, *Proceedings of the 8th Symposium on Thermophysical Properties. American Society of Mechanical Engineers (ASME)*; New York 1982, pp. 422–428.
[27] E.U. Mapesa, M. Tarnacka, E. Kamińska, K. Adrjanowicz, M. Dulski, W. Kossack, M. Tress, W.K. Kipnusu, K. Kamiński, F. Kremer, Molecular dynamics of itraconazole confined in thin supported layers, RSC Adv. 4 (54) (2014) 28432–28438, https://doi.org/10.1039/c4ra01544d.
[28] M. Tarnacka, K. Adrjanowicz, E. Kaminska, K. Kaminski, K. Grzybowska, K. Kolodziejczyk, P. Wlodarczyk, L. Hawelek, G. Garbacz, A. Kocot, et al., Molecular dynamics of itraconazole at ambient and high pressure, Phys. Chem. Chem. Phys. 15 (47) (2013) 20742–20752, https://doi.org/10.1039/c3cp52643g.
[29] K.P. Sigdel, G.S. Iannacchione, Study of the isotropic to smectic-a phase transition in liquid crystal and acetone binary mixtures, J. Chem. Phys. 133 (17) (2010), 174501, https://doi.org/10.1063/1.3502112.
[30] P.R. Couchman, F.E. Karasz, A classical thermodynamic discussion of the effect of composition on glass-transition temperatures, Macromolecules 11 (1) (1978) 117–119, https://doi.org/10.1021/ma60061a021.
[31] T.G. Fox, P.J. Flory, On a general relation involving the glass temperature and coefficients of expansion of, Glas. Transit. J. Chem. Phys. 21 (March 1962) (1950) 1003, https://doi.org/10.1063/1.1699711.
[32] M. Gordon, J.S. Taylor, Ideal copolymers and the second-order transitions of synthetic rubbers. I. Noncrystalline copolymers, Rubber Chem. Technol. 26 (2) (2011) 323–335, https://doi.org/10.5254/1.3539818.
[33] B.C. Hancock, G. Zografi, The relationship between the glass transition temperature and the water content of amorphous pharmaceutical solids, Pharm. Res. 11 (4) (1994) 471–477, https://doi.org/10.1023/A:1018941810744.
[34] H.-M. Philp Chen, J.J. Ou, S.H. Chen, Glassy liquid crystals as self-organized films for robust optoelectronic devices, in: Q. Li (Ed.), Nanoscience With Liquid Crystals, Springer International Publishing 2014, pp. 179–208, https://doi.org/10.1007/978-3-319-04867-3_6.
[35] K. Denolf, B. Van Roie, C. Glorieux, J. Thoen, Effect of nonmesogenic impurities on the order of the nematic to smectic-a phase transition in liquid crystals, Phys. Rev. Lett. 97 (10) (2006) 1–4, https://doi.org/10.1103/PhysRevLett.97.107801.
[36] P.M. Chaikin, T.C. Lubensky, Principles of Condensed Matter Physics, Cambridge University Press, 1995https://doi.org/10.1017/CBO9780511813467.